Crystal Structure of Carbon Dioxide at High Pressure: "Superhard" Polymeric Carbon Dioxide

C. S. Yoo,[1] H. Cynn,[1] F. Gygi,[1] G. Galli,[1] V. Iota,[1] M. Nicol,[2] S. Carlson,[3] D. Häusermann,[3] and C. Mailhiot[1]
[1]*Lawrence Livermore National Laboratory, Livermore, California 94551*
[2]*High Pressure Science Center at University of Nevada, Las Vegas, Nevada 89154*
[3]*European Synchrotron Radiation Facility, Grenoble, France*
(Received 16 June 1999)

The crystal structures of two molecular phases (I and III) and a polymeric phase (V) of CO_2 have been investigated to 60 GPa. CO_2-I ($Pa3$) transforms to CO_2-III ($Cmca$) at 12 GPa with almost no change of density. Although CO_2-III persists in $Cmca$ to at least 60 GPa at ambient temperature, it transforms when heated to 1800 K above 40 GPa to tridymite ($P2_12_12_1$) CO_2-V with 15.3% volume change. Each carbon atom of CO_2-V is tetrahedrally bonded to four oxygen atoms. CO_2-V is likely superhard with low compressibility $B_0 = 365$ GPa, similar to cubic BN.

PACS numbers: 64.70.Kb, 62.50.+p, 71.15.Nc, 81.05.Lg

Simple molecular solids are described in terms of strong covalent bonds within molecules and weak van der Waals interactions between molecules. The strong intramolecular bonds make these molecules extremely stable at ambient conditions, whereas the weak intermolecular interactions make their crystals very soft, at least initially at relatively low pressures. At high pressures, however, the nature of these intermolecular interactions rapidly alters and becomes highly repulsive. Electron kinetic energy dominates; electrons localized within intramolecular bonds become unstable. Under these circumstances, molecular solids should undergo physical and chemical changes to modify the chemical bonds and to soften the stiff repulsive intermolecular potential. Ionization, polymerization, and metallization are mechanisms by which molecular solids may delocalize electrons at high pressures, as observed in many covalent solids like CO_2 [1], N_2 [2], CO [3,4], O_2 [5], and C_2N_2 [6].

Five carbon dioxide polymorphs have been reported at high pressures: four (CO_2-I to CO_2-IV) molecular solids [7–10] and a recently discovered polymeric CO_2-V phase [1]. At 298 K and 1.5 GPa, CO_2 crystallizes as the cubic $Pa3$ phase I [7]. CO_2-I transforms to an orthorhombic $Cmca$ phase CO_2-III between 10 and 20 GPa [9,10]. The I-III phase boundary is not well characterized. Raman studies [10] suggest that CO_2-III appears above 20 GPa, and a "distorted" phase CO_2-IV coexists with CO_2-I between 11 and 20 GPa. In contrast, a crystal structure of CO_2-III was determined from the mixtures of CO_2-I and CO_2-III between 8 and 12 GPa [9]. The crystal structure of CO_2-III has not been determined above 12 GPa nor from the single phase of CO_2-III. Recently, we discovered that CO_2-III transforms to a new optically nonlinear phase CO_2-V above 40 GPa upon heating to 1800 K [1], the vibrational characteristics of which are analogous to SiO_2. The crystal structure of this novel CO_2-V has not been determined as yet.

In this Letter, we report (i) the crystal structure of CO_2-V is indeed similar to SiO_2-tridymite ($P2_12_12_1$). (ii) CO_2-V is likely superhard like cubic-BN. (iii) CO_2-III remains in $Cmca$ up to 60 GPa at ambient temperature, although it may not be a typical molecular solid.

Carbon dioxide samples were prepared by condensing CO_2 gas at $-40\,^\circ$C and 10 bars into diamond-anvil cells (DAC's). A few micrometer-size ruby chips scattered inside the DAC provided *in situ* measures of the pressures at several locations of the sample. CO_2-V was synthesized by indirectly heating CO_2-III at high pressures between 20 and 50 GPa above 1800 K and as high as 3000 K by irradiating the ruby using a Nd:YLF (yttrium lithium fluoride) laser [1]. The crystal structures of the CO_2 phases were determined by angle-resolved x-ray diffraction using focused monochromatic ($\lambda = 0.3738$ Å) x-ray at the European Synchrotron Radiation Facility. With a 10 μm diameter pinhole collimator, we could isolate the incident x ray on a single phase region of the sample to obtain the patterns shown here. The diffraction patterns were recorded on a fast scanning image plate and were analyzed by using a FIT2D program [11]. Because of highly preferred orientations of the CO_2 phases, especially phase III, the DAC were rotated around an axis perpendicular to the incident x-ray beam during exposure to obtain high quality diffraction patterns.

The visual appearance of CO_2 phases is quite distinctive (Fig. 1). CO_2-I at 6.7 GPa (a) is an isotropic cubic crystal, showing no grain boundaries despite its high polycrystallinity. In contrast, CO_2-III at 32.8 GPa (b) shows several grain boundaries of large crystallites with very characteristic textures of a highly strained lattice. Pressure gradients measured over the CO_2-III samples are large, from 100 to 200 GPa mm^{-1} at pressures above 30 GPa. That is, the pressure at the center of a CO_2-III sample could be 10 or more GPa greater than at the edge; these gradients are unusually large for "soft" molecular crystals. Both the textures and large pressure gradients indicate that CO_2-III is a high-strength material at these pressures. Above 40 GPa, CO_2-III transforms at 1800 K to CO_2-V that can be quenched to ambient temperature.

0031-9007/99/83(26)/5527(4)$15.00

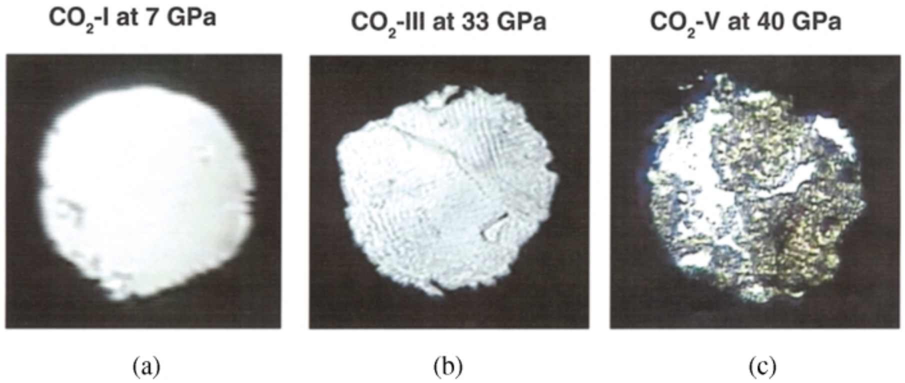

FIG. 1 (color). Microphotographs of CO_2 phases at high pressures: (a) CO_2-I at 6.7 GPa, (b) CO_2-III at 32.8 GPa, and (c) CO_2-V at 40 GPa. The samples are approximately 100 μm in diameter.

Quenched CO_2-V at 40 GPa (c) is highly polycrystalline, as distinct from the untransformed phase III.

The x-ray diffraction pattern for CO_2-I (Fig. 2) is readily indexed as a $Pa3$ structure with four molecules per unit cell, consistent with previous assignments [7,9]. The diffraction peaks of CO_2-III are extremely broad because of the large pressure gradient mentioned above. Nevertheless, the measured and calculated diffraction patterns of CO_2-III agree reasonably well within a $Cmca$ cell. In the $Pa3$ structure, the carbon atoms of CO_2 molecules are on the face-centered positions with their molecular axes aligned along body diagonals. The carbon atoms in the $Cmca$ remain face centered, but all CO_2 molecules are aligned parallel to the bc-basal plane with their molecular axes tilted by about 52° from the c axis as previously described [9].

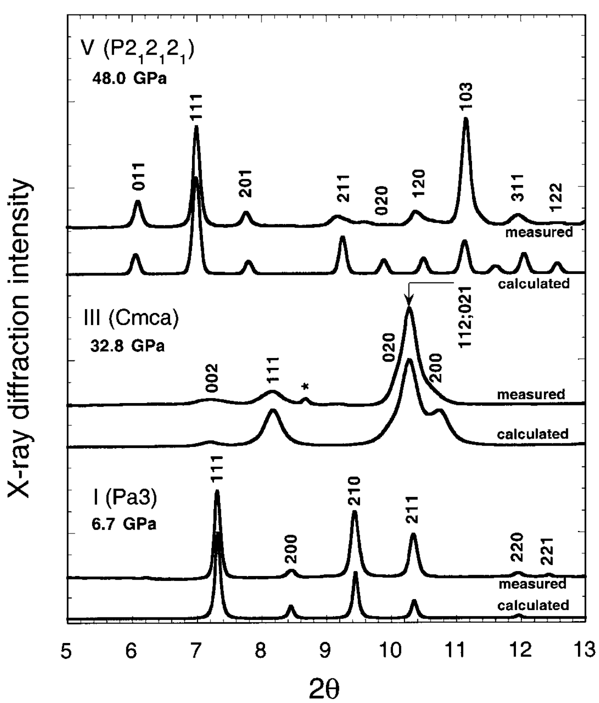

FIG. 2. Observed and calculated angle-resolved x-ray diffraction patterns of CO_2 phases. The small peak marked with an asterisk is from the gasket.

The diffraction pattern of CO_2-V can be fitted in terms of an orthorhombic structure with lattice parameters, $a = 6.216$ Å, $b = 4.352$ Å, $c = 6.066$ Å at 48 GPa, consistent with 8 molecules per unit cell (Table I). The intensity data and evidence for preferred orientation do not allow rigorous refinement of the structure. Nevertheless, we found a reasonable description of the diffraction pattern in terms of SiO_2-tridymite structures, particularly with an orthorhombic $P2_12_12_1$ structure that represents about $1/3$ of a known SiO_2-tridymite unit cell [12,13]. The difference in the measured and calculated diffraction intensities is notable particularly for the 103 reflection, probably due to the preferred orientation and/or disorder in the oxygen sublattice of the tridymite structure [14]. In fact, we have verified that introducing a slight disorder into the oxygen positions increases the intensity of the 103 reflection and makes it the strongest.

All tridymite structures can be derived from a parent hexagonal ($P6_3/mmc$) structure, a high temperature modification of β-SiO_2 quartz ($P6222_1$), by appropriate rotations of CO_4 tetrahedra [13,14]. In this "ideal" $P2_12_12_1$ tridymite structure of CO_2-V, each carbon atom is tetrahedrally bound to four oxygen atoms with the carbon-oxygen bond distances between 1.34(0.01) at 60 GPa and 1.40(0.01) Å at 10 GPa. The O-C-O angles are estimated to be 110(10)° (Fig. 3). These CO_4 tetrahedral units share their corner oxygens to form sixfold distorted holohedral rings with alternating tetrahedral apices pointing up

TABLE I. The crystal structure of CO_2-V ($P2_12_12_1$) at 48 GPa: $a = 6.216$ Å, $b = 4.352$ Å, $c = 6.066$ Å, and $\rho = 3.561$ g/cm^3.

hkl	d_{cal}(Å)	I_{cal}	d_{obs}(Å)	I_{obs}	Δd(Å)
011; 110	3.536	20	3.531	27	0.005
111; 200; 002	3.074	100	3.066	96	0.008
201	2.766	13	2.766	17	0.000
211; 112	2.335	37	2.334	14	0.001
202; 020	2.171	14	2.161	3	0.010
120; 021	2.054	17	2.058	18	−0.004
103; 301; 310	1.923	33	1.923	100	0.001
311	1.788	20	1.793	14	−0.005
122; 203	1.701	12	1.700	2	0.001

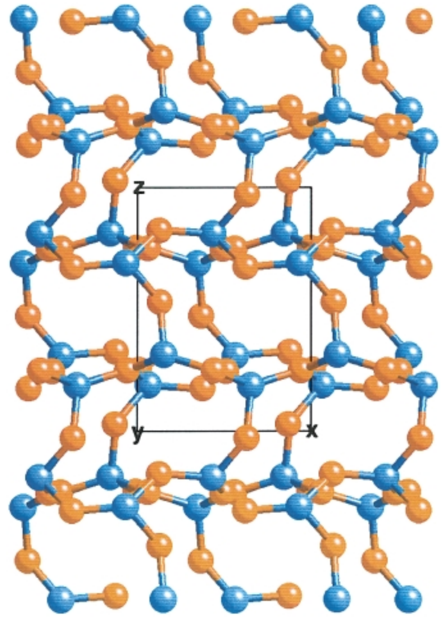

FIG. 3 (color). An "ideal" crystal structure of CO_2-V in $P2_12_12_1$ with 8 molecules per unit cells. Carbon atoms (blue) are tetrahedrally bonded to four oxygen atoms (red). Those CO_4 tetrahedra form a layer in the *ab* plane; the apices are connected through oxygen atoms along the *c* axis.

and down the *ab* plane. The apices of tetrahedra are then connected through oxygen atoms along the *c* axis. This interconnected layer structure of tetrahedra yields the C-O-C angle 130(10)°, substantially smaller than those of SiO_2-tridymites, 174°–180°.

CO_2-V is clearly metastable at ambient temperatures over a large pressure range including the entire stability field of CO_2-III (Fig. 4). Below 10 GPa, CO_2-V begins to depolymerize to CO_2-I; however, diffraction peaks of CO_2-V remain even at 4 GPa. This observation is consistent with earlier Raman data showing the C-O-C vibrational band above 1 GPa [1].

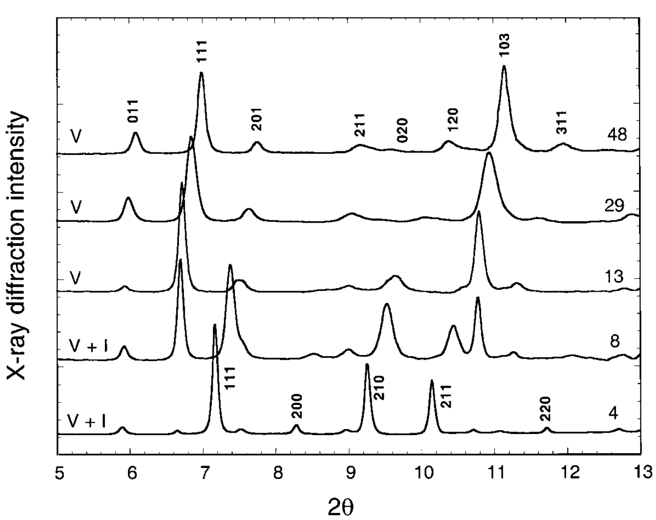

FIG. 4. Angle-resolved x-ray diffraction patterns of CO_2-V at several high pressures. The numbers indicate the pressures in GPa.

CO_2-I transforms to CO_2-III at 12 GPa with no apparent volume discontinuity (Fig. 5). The x-ray diffraction patterns between 10 and 20 GPa can be fit in terms of CO_2-I and CO_2-III; no features are apparent for CO_2-IV. This may mean that the structure of CO_2-IV is similar to that of CO_2-III as suggested by the description, "distorted CO_2-III," used in earlier Raman studies [10]. The volume changes associated with this molecular-to-extended (III-to-V) transition vary between 15.3% at 40 GPa and 12.6% at 60 GPa, at ambient temperatures. Extrapolations of CO_2-V and CO_2-III data yield the volumes 0.322 and 0.453 cm^3/g, respectively.

The stability and bulk properties of various candidate structures of CO_2-V have been investigated by using *ab initio* quantum molecular dynamics simulations [15] within density functional theory [16]. Both the ionic forces and the stress tensor were calculated and updated using a simulated annealing scheme until full relaxation of ionic positions and cell geometry were obtained. After analyzing several structures derived from known crystalline phases of SiO_2, we found tridymite structures to be among the most stable structures, being energetically close in some cases lower than α quartz, β quartz, and cristobalite. The recently proposed *m*-chacopyrite structure [17] was also investigated. The calculated enthalpy of the relaxed *m*-chacopyrite structure at 40 GPa is very similar to those of the other tridymites and quartz structures, all of which values are grouped in an energy interval of 1.5 eV/molecule [18]. However, the calculated powder diffraction pattern of an orthorhombic $P2_12_12_1$ tridymite gives the best account of experimental data, whereas other structures conspicuously lack several observed diffraction peaks. Calculated volumes (solid circles in Fig. 5) agree reasonably well with the

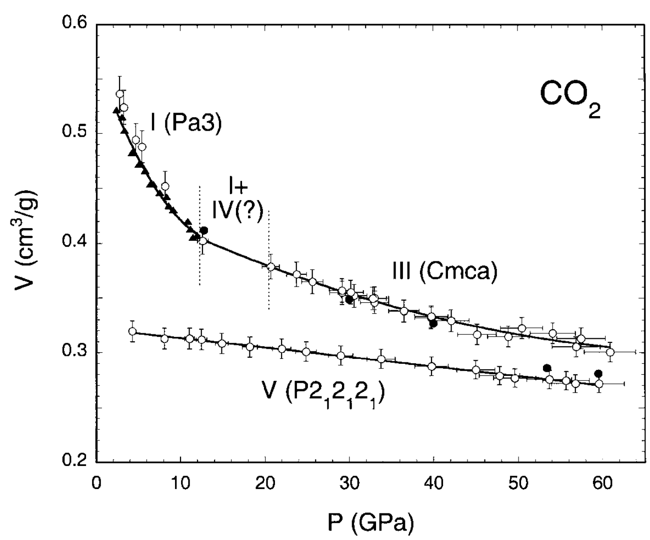

FIG. 5. Pressure-volume relations of CO_2 phases. The open circles with error bars are the measured specific volumes in this study; the solid triangles are from [7]. The calculated volumes of CO_2-III and CO_2-V are also shown as the solid circles. The Birch-Murnaghan fits (lines) yield $B_0 = 365$ GPa for CO_2-V, 87 GPa for CO_2-III, and 12 GPa for CO_2-I.

experimental ones. The volumes of CO_2-I and CO_2-III, on the other hand, were calculated by using a classical method [19], which also yields a good agreement with the measured ones within the estimated errors.

CO_2-I is soft, but both CO_2-III and CO_2-V are very stiff solids (Fig. 5). The bulk modulus B_0 of CO_2-I is 12.4 GPa typical for a molecular solid. In contrast, the B_0 of CO_2-III is unusually high 87 GPa, nearly in the range of Si (98 GPa) [20]. This result is consistent with the pressure gradient and observed texture in CO_2-III. Furthermore, the nearest neighbor C-O distance collapses to 2.303 Å at 40 GPa, from 3.135 Å at 1.5 GPa. These imply that CO_2-III is not entirely molecular; that is, the intermolecular bonding between neighboring CO_2 molecules is substantial. Such increased intermolecular bonding in CO_2-III at high pressures will certainly increase the strength of this material and act as a precursor for the transition to an extended phase like CO_2-V. The B_0 of CO_2-V (365 GPa) is much higher than that of SiO_2 quartz (37 GPa) or even stishovite (310 GPa) and is comparable to that of cubic-BN (369 GPa) [20]. This high bulk modulus and the large pressure gradient that CO_2-V supports lead us to conjecture that CO_2-V is a superhard polymer.

The I-III transformation can be described in terms of simple molecular reorientation from along a body diagonal into the basal plane. This involves relatively small atomic displacement and thus occurs martensitically. Martensitic transitions are typically driven mechanically by shear and often are accompanied by large hysteresis of the transition and/or lattice distortions [21]. The coexistence of CO_2-I and CO_2-III over a relatively large pressure region reflects the sluggish nature of such a mechanically driven transition. In fact, we found that annealing the mixtures of CO_2-I and CO_2-III (or CO_2-IV) at high temperatures completely transforms CO_2-I to CO_2-III (or CO_2-IV) at 11 GPa without hysteresis. Attractive intermolecular interactions in CO_2-III would soften the steep repulsive potential and prolong the stability field of CO_2-III to well above 40 GPa at ambient temperature. The transition from CO_2-III to CO_2-V, on the other hand, is reconstructive and driven by the large energy reduction that results from forming the three-dimensional network of chemical bonds. Heating is required to overcome a high activation barrier between the CO_2-III and CO_2-V structures. The high activation barrier and density of CO_2-V account for the metastability of this phase over a wide range of pressures at low temperatures.

It is well known that in SiO_2 there is very little energy difference for various polymorphs of tridymite [12]. In addition, there often exists a substantial distortion in the oxygen sublattice of SiO_2-tridymite [14]. However, all C-O-C angles in CO_2-V were estimated to be about 130°, contrary to a wide range of Si-O-Si angles in SiO_2 from near 180° in tridymite to 145° in quartz. Such rigidity in the C-O-C angle results in a relatively large distortion in the sixfold holohedra along the ab plane of CO_2-V. It in turn reflects the fact that oxygen atoms in CO_2-V are more tightly bound than in SiO_2 and results in a higher covalence and bulk modulus of CO_2-V than of any SiO_2 polymorphs.

The x-ray diffraction studies were done at ESRF and SSRL. We appreciate K. Visbeck and L. Yang for their contribution. This work has been supported by the LDRD under the auspices of the DOE under the Contracts No. W-7405-ENG-48 and No. DE-FC08-98NV13410.

[1] V. Iota, C. S. Yoo, and H. Cynn, Science **283**, 1510 (1999).
[2] C. Mailhiot, L. H. Yang, and A. K. McMahan, Phys. Rev. B **46**, 14 419 (1992).
[3] A. Katz, D. Schiferl, and R. L. Mills, J. Phys. Chem. **88**, 3176 (1984).
[4] S. Bernard, G. L. Charity, S. Scandolo, and E. Tosatti, Phys. Rev. Lett. **81**, 2092 (1998).
[5] S. Desgreniers, Y. K. Vohra, and A. L. Ruoff, J. Phys. Chem. **94**, 1117 (1990).
[6] C. S. Yoo and M. F. Nicol, J. Phys. Chem. **90**, 6726 (1986); **90**, 6732 (1986).
[7] B. Olinger, J. Chem. Phys. **77**, 6255 (1982).
[8] L. Liu, Nature (London) **303**, 508 (1983).
[9] K. Aoki, H. Yamawaki, M. Sakashita, Y. Gotoh, and K. Takemura, Science **263**, 356 (1994).
[10] H. Olijnyk and A. P. Jephcoat, Phys. Rev. B **57**, 879 (1998).
[11] A. P. Hammersley, *FIT2D V9.I29 Reference manual v3.1,* ESRF Report No. 98HA01T, 1998.
[12] A. K. A. Pryde and M. T. Dove, Phys. Chem. Miner. **26**, 171 (1998).
[13] R. F. de Dombal and M. A. Carpenter, Eur. J. Mineral **5**, 607 (1993), and references therein.
[14] H. Graetsch and O. W. Flörke, Z. Kristallogr. **195**, 31 (1991).
[15] G. Gali and A. Pasquarello, in *Computer Simulation in Chemical Physics*, edited by M. P. Allen and D. J. Tildesley, NATO ASI, Ser. C, Vol. 397 (Kluwer, Dordrecht, 1993), p. 261.
[16] We used JEEP 1.4.7 code written by F. Gygi, using nonlocal, norm-conserving pseudopotentials [D. R. Hamann, Phys. Rev. B **55**, 10 157 (1997)] and the generalized gradient approximation [J. P. Perdew, K. Burke, and M. Ernzerhof, Phys. Rev. Lett. **77**, 3865 (1996)].
[17] S. Serra, C. Cavazzoni, G. L. Chiarotti, S. Scandolo, and E. Tosatti, Science **284**, 788 (1999).
[18] We find that the tetragonal cell describing the m-chacopyrite undergoes a strong relaxation of its c/a to 1.5, a significant deviation from the ideal value 2. This induces important changes in the C-O-C and O-C-O angles, departing from the ideal tetrahedral 109.5°.
[19] G. Steinebrunner, A. J. Dyson, B. Kirchner, and H. Huber, J. Chem. Phys. **109**, 3153 (1998).
[20] E. Knittle, *Mineral Physics and Crystallography, a Handbook of Physical Constants,* edited by T. Ahrens (AGU, Washington, DC, 1995), pp. 98–142; E. Knittle *et al.*, Nature (London) **337**, 349 (1989).
[21] D. Pandey and S. Lee, Acta Metall. **34**, 405 (1986).